

A NEW APPROACH TO SPHERICALLY SYMMETRIC JUNCTION SURFACES AND THE MATCHING OF FLRW REGIONS

U Kirchner

Department of Mathematics and Applied Mathematics
 University of Cape Town
 7700 Rondebosch, South Africa
 e-mail: uli@maths.uct.ac.za

30. November 2003

Abstract

We investigate timelike junctions (with surface layer) between spherically symmetric solutions of the Einstein-field equation. In contrast to previous investigations this is done in a coordinate system in which the junction surface motion is absorbed in the metric, while all coordinates are continuous at the junction surface.

The evolution equations for all relevant quantities are derived. We discuss the no-surface layer case (boundary surface) and study the behaviour for small surface energies. It is shown that one should expect cases in which the speed of light is reached within a finite proper time.

We carefully discuss necessary and sufficient conditions for a possible matching of spherically symmetric sections.

For timelike junctions between spherically symmetric space-time sections we show explicitly that the time component of the Lanczos equation always reduces to an identity (independently of the surface equation of state).

The results are applied to the matching of FLRW models. We discuss ‘vacuum bubbles’ and closed-open junctions in detail. As illustrations several numerical integration results are presented, some of them indicate that the junction surface can reach the speed of light within a finite time.

1 Introduction

Recent measurements of the microwave background radiation support the idea that our universe is highly isotropic and homogeneous [1]. Cosmological models with these properties are uniquely represented by the class of Friedmann-Lemaître-Robertson-Walker (FLRW) models. The observed flatness of the universe can then be explained by employing an inflationary model [2], which suggests an exponential expansion of the early universe driven by a scalar field – the inflaton field.

Nevertheless, it is often speculated that this might only be the local geometry, while over a larger scale the universe is inhomogeneous and anisotropic, i.e., the matter content and geometry vary. In particular, it appears as if the parameters necessary for life are highly fine-tuned and in order to solve this “fine-tuning problem” it was suggested that we live in one of many different FLRW regions – most of them might be unsuitable for life. The most prominent example is Linde’s Chaotic Inflation Scenario [3, 4], in which the different FLRW regions originate from different almost homogeneous Planck-sized regions which experience a period of exponential expansion.

When such models are discussed it is usually assumed that the transition region between two almost FLRW regions is very small and can be approximated by a timelike junction hypersurface, the so-called thin bubble wall. To find the motion of this hypersurface one has to find the matching surface to the two solutions of the Einstein-field equation representing the space-time on each side.

The matching conditions are of two different types. On the one hand there is the purely geometric necessity that ‘things fit together’ — distances on the junction surface should have the same length when measured ‘inside’ or ‘outside’. On a mathematical level this reduces to a matching of the tangential metric components.

On the other hand there are the matching conditions which result from the assumed validity of certain physical laws, in particular the energy-momentum conservation across the junction surface and the validity of the Einstein-field equation on each side. These conditions have been evaluated by C. Lanczos [5], R. Dautcourt [6], and in a ground-breaking work by W. Israel [7].

While these equations are in principle valid for any matching of two space-times satisfying the Einstein-field equation, it is in practice impossible to handle their complexity except for highly symmetric cases and for all practical applications spherical symmetry is assumed. There is a vast amount of literature, see e.g., [7, 8, 9, 10].

A good introduction to the standard method for dealing with spherically symmetric junctions is given by K. Lake in [10], where also different matchings, including cosmological voids and vacuum bubbles, are studied numerically. In [9] V. A. Berezin, V. A. Kuzmin and I. I. Tkachev considered the generic spherically symmetric case and expressed the relevant quantities with invariants. Junctions arising from phase transitions in the early universe, including junctions between sections of FLRW sections are discussed.

Our aim here is to present a new approach to junctions between spherically symmetric space-times and to apply the formalism to junctions between FLRW models — analytically and numerically.

The approach will focus on the geometrical quantities describing the situation, i.e., the distance of the junction surface from the centre of symmetry, and not alone on the junction surface radius. In contrast to most other studies, we do not evaluate the junction conditions (in particular the Lanczos equation) in the original coordinate system or in Gaussian normal coordinates based on the junction surface. Instead we introduce new coordinates such that the junction surface is at a fixed (new) “radial” coordinate and all coordinates are continuous at the junction surface. The motion of the junction surface is now absorbed into the metric components.

In spherically symmetric cases the Lanczos equation has two non-trivial independent components – an angular and a time component. While the first one leads to the well-known evolution equations, there seems to be uncertainty about the interpretation of the time component, which is a second order (in time) differential equation for the junction surface motion. It has been known that for certain particular cases this equation reduces to an identity [11]. Nevertheless, other authors¹ suggested that this equation acts as a surface equation of state [9], i.e., determines the surface pressure. Using the presented approach we will show that the time component of the Lanczos equation is in fact an identity for all junctions between spherically symmetric solutions of the Einstein-field equation.

It should be pointed out that there are special cases of junctions which could be examined without employing junction conditions. If the γ -equation of state and the cosmological constant have no discontinuity at the junction surface then the spherically symmetric space-time can be described in terms of the Lemaître-Tolman model. However, the really interesting question is how the junction behaves if the inside and outside region have different dynamical behaviour, i.e., different equation of state and cosmological constant. For these cases one cannot avoid the use of junction conditions and all numerical examples given in this paper will be of this kind.

Our approach differs in the use of a coordinate transformation to minimize the number of discontinuous quantities and to evaluate the standard junction conditions in a more convenient form (leading to (23) and (24)). The main results do agree with well known results in the literature — for example the evolution equation for the angular metric component (30) can be found in a similar (though I believe less convenient) form in [10] and the results for vacuum bubbles agree with findings in [9] and [12].

This paper will be structured as follows: In section 2 we re-examine junction conditions for the matching of generic spherically symmetric sections. We will re-derive the evolution and constraint equations using a new approach, based on a coordinate transformation which makes *all* coordinates continuous at the junction surface. We investigate the behaviour for small values of the surface-energy density and discuss the special case of vanishing surface-energy density. In section 3 we pay particular attention to constraints on the surface-energy density and in section 4 we show that the time-component of the Lanczos equation is an identity. This is followed by an application to the matching of FLRW sections in section 5 and three numerical examples in section 6.

1.1 Notation

We use standard notation and metric signature $(-+++)$. Coordinates are labeled with greek indices, running from 0 to 3, where 0 represents the time coordinate. Latin indices label coordinates on the three-dimensional

¹In particular this was suggested for the junction between FLRW models.

junction hypersurface. As will be seen below, with our choice of coordinates the junction surface is located at a fixed radial coordinate $R = 1$, and hence latin indices take the values 0, 2, and 3 (or equivalently t, θ , and ϕ).

When considering quantities defined for certain hypersurfaces (like the junction surface) it will be convenient to have a covariant derivative for this subspace. We will use a vertical bar (like in $K_{ab|c}$) to refer to this covariant hypersurface derivative, which is evaluated in the same way as above covariant derivative, but with all quantities replaced by the corresponding hypersurface quantities. Any quantity referring to the three-dimensional hypersurface of the junction surface will have a superscript ‘(3)’, e.g., ${}^{(3)}R$ and ${}^{(3)}g_{ab}$.

We will use a subscript – or + sign to indicate whether quantities refer to the in- or outside region, respectively.

2 Matching of generic O(3)-symmetric sections

2.1 The coordinate system

Any spherically symmetric space-time (i.e., having O(3) symmetry) allows coordinates such that the metric takes the form

$$ds^2 = -\mathfrak{N}^2(\tau, r)d\tau^2 + l^2(\tau, r)\{dr^2 + f^2(\tau, r)d\Omega^2\}, \quad (1)$$

where $\mathfrak{N}(\tau, r)$ is the so-called lapse function, and $d\Omega^2 = d\theta^2 + \sin^2(\theta)d\phi^2$ the line-element on the two-dimensional unit-sphere.

We are interested in the matching of two spherically symmetric space-times, each having a metric of the form (1). Generally, the coordinates will not match up at the junction surface and the manifold is described by two different coordinate charts – one for the inside region (subscript –) and one for the outside region (subscript +). At any coordinate time (in the inside or outside region) the junction surface itself is assumed to be a two-sphere which is described by its coordinate radius in the inside and outside region, $\alpha_-(\tau_-)$ and $\alpha_+(\tau_+)$.

Since the inside and outside regions are originally described by a metric in the form (1) we will use the convention that a dot/prime refers to the proper time/radial derivative with respect to the metric (1) at the junction surface, e.g.,

$$i_+ \stackrel{\text{def}}{=} \frac{1}{\mathfrak{N}_+} \frac{\partial}{\partial \tau} l_+(\tau, r) \Big|_{r=\alpha_+(\tau_+)} \quad \text{and} \quad l'_+ \stackrel{\text{def}}{=} \frac{1}{l_+} \frac{\partial}{\partial r} l_+(\tau, r) \Big|_{r=\alpha_+(\tau_+)}.$$

In order to describe the motion of the junction surface one usually tries to find the evolution of the junction surface radius in each coordinate system. Here we want to suggest a different approach: we introduce a new coordinate system, such that *all* the coordinates are continuous at the junction surface while only the transverse metric components are discontinuous at the junction surface. The junction surface motion is now described by the evolution of the metric components.

This, however, should not be confused with Gaussian normal coordinates (which are widely used in the discussion of junctions) as our coordinate curves $x^\mu = \text{const.}$ will be in general non-orthogonal at the junction.

Constructing a continuous time coordinate Let us assume that the inside and outside spaces are given in terms of their metrics, which take the form (1). Generally the time coordinates for the inside and outside region will not match up at the junction hypersurface.

Since the junction surface is timelike, each value of the time-coordinate (in the inside or outside region) identifies a unique spherically symmetric hypersurface of the junction. This establishes a strictly monotonically increasing one-to-one relation between the times on each side $\tau_+ = F(\tau_-)$. Setting $d\tau_- \stackrel{\text{def}}{=} t$, $d\tau_+ \stackrel{\text{def}}{=} F'(t)dt$ introduces the new continuous ‘global time coordinate’ t . This rescaling is independent of r and leaves the form of the metric (1) invariant. However, if the original lapse function was constant then this re-scaling results in a new time dependent lapse function which contains information about the junction surface motion. For example, this will be the case for the matching of FLRW models.

If on the other hand the original lapse function $\mathfrak{N}(\tau, r)$, where τ is the original time coordinate, depends on the radial coordinate then we can write the new lapse function (which makes the time coordinate continuous) as

$$N(t, r) = F'(t)\mathfrak{N}(\tau, r),$$

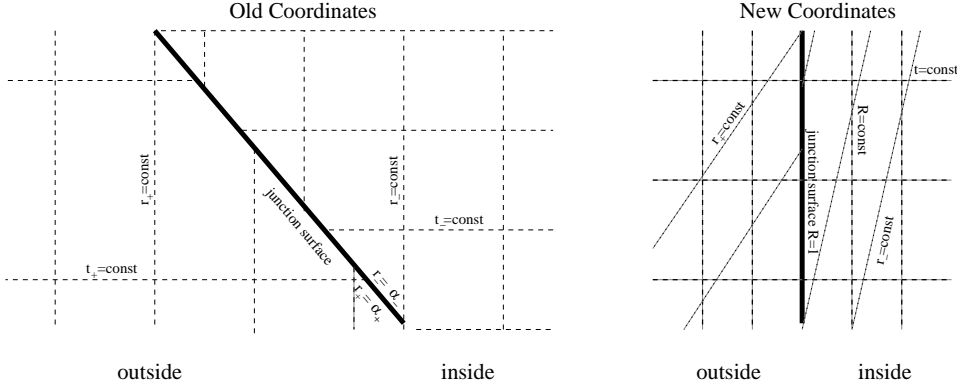


Figure 1: An illustration of the coordinate transformation. The original radial coordinates r_+ and r_- are rescaled such that in the new coordinate system the junction surface is at a fixed ‘radial’ coordinate $R = 1$. The time-coordinates are rescaled such that they match up at the junction surface.

where $\tau = \int_0^t F'(t')dt'$ and t is the new time coordinate. It is now $\eta(t)$ which contains information about the junction surface motion, while \mathfrak{N} contains information about the background space. In particular, the quantity

$$\frac{N'(t, r)}{N(t, r)} = \frac{\mathfrak{N}'(\tau, r)}{\mathfrak{N}(\tau, r)}$$

(taken as a function of proper time) does not depend on F' . We will keep these issues in mind when we use the lapse function in the following calculations.

Finally it should be pointed out that there remains the ‘gauge freedom’ to rescale the new global time-coordinate t , which will be used later.

Constructing a continuous radial coordinate Now we want to construct new radial coordinates such that the junction surface is at a fixed radial coordinate $R = 1$. This can be achieved by setting $r_{\pm} = \alpha_{\pm}(t)R$, where the subscript $+$ refers to outside ($R > 1$) and $-$ to the inside region, and $\alpha_{\pm}(t)$ is the coordinate radius of the junction surface at time t . The relation between the old and the new coordinates is illustrated in figure 1. With this new radial coordinate the metrics for the inside and outside region take the form

$$ds^2 = -N^2\{1 - R^2\dot{\alpha}^2l^2\}dt^2 + 2\alpha N\dot{\alpha}l^2RdR dt + l^2\{\alpha^2dR^2 + f^2(\alpha R)d\Omega^2\}, \quad (2)$$

where a dot indicates the proper time derivative along paths of constant r, θ, ϕ , i.e., $\dot{\alpha} \stackrel{\text{def}}{=} \frac{1}{N} \frac{\partial}{\partial t} \alpha$.

2.2 Geometric matching conditions

At the matching surface $R = 1$ the tangential metric components must be continuous. This gives us the two matching conditions

$$[lf] = 0. \quad (3)$$

and

$$[N^2(\dot{\alpha}^2l^2 - 1)] = 0, \quad (4)$$

where

$$[g(R)] \stackrel{\text{def}}{=} \lim_{R \rightarrow 1^+} (g(R)) - \lim_{R \rightarrow 1^-} (g(R)) = \lim_{r_+ \rightarrow \alpha_+(t)^+} (g_+(r_+)) - \lim_{r_- \rightarrow \alpha_-(t)^-} (g_-(r_-)).$$

These relations identify two quantities which are continuous across the junction surface and we define

$$k(t, R) \stackrel{\text{def}}{=} N\sqrt{1 - \dot{\alpha}^2l^2R^2} \quad , \quad k \stackrel{\text{def}}{=} k(t, 1) = N\sqrt{1 - \dot{\alpha}^2l^2} \Big|_{R=1} \quad (5)$$

and

$$w \stackrel{\text{def}}{=} lf, \quad (6)$$

which are the tangential metric components. Note that $k(t, R)$ becomes complex for large $\dot{\alpha}^2 l^2 R^2$. However, this is not of relevance for the problem at hand, since we are only interested in the behaviour around the junction surface at $R = 1$ where $k(t, R)$ is real for timelike junction surfaces.

It follows from (4) that if the surface appears from one side as timelike, it will so from the other side. From now on let us assume that the junction surface is a timelike surface, *i.e.*, $\dot{\alpha}_\pm l_\pm < 1$.

There is a remaining gauge freedom: we can rescale the global time coordinate, *i.e.*, multiply the lapse functions with a time dependent factor. One particularly useful choice is to rescale the time such that the tangential metric component in the timelike direction parallel to the junction surface becomes unity, *i.e.*,

$$k = N \sqrt{1 - \dot{\alpha}^2 l^2} \Big|_{R=1} = 1. \quad (7)$$

To maintain generality we will not assume this choice until explicitly stated (in section 2.4).

The two conditions (3) and (4) are of pure geometric character – they have to be satisfied independently of the evolution equations at all times. Taking the total derivative of (6) with respect to coordinate time we obtain the corresponding restriction on the junction surface motion

$$\frac{dw}{dt} = N \{(lf)^\bullet + (lf)' \dot{\alpha} l\} \quad \left[\frac{dw}{dt} \right] = 0. \quad (8)$$

It should be noted that here N is not independent, but depends via (7) on the junction surface motion. Equations (7) and (8) generally have two solutions for the junction surface motion in terms of the surface radius evolution.

Let us note here that the metric of the timelike hypersurface representing the junction surface is given by

$${}^{(3)}g_{\mu\nu} dx^\mu dx^\nu \stackrel{\text{def}}{=} ds_\Sigma^2 = -k^2 dt^2 + w^2 d\Omega^2.$$

The intrinsic geometry of the junction hypersurface is completely defined by k and w . Nevertheless, w might not uniquely identify the position of the junction surface. Only if $l_+ f_+$ and $l_- f_-$ are invertible functions of α_\pm then the position of the junction surface is indirectly given by the value of w .

2.3 Lanczos equation and Israel junction conditions

Let us split the energy-momentum tensor in a regular and a δ -function part, so that

$$T_{\mu\nu} = \delta(\eta) S_{\mu\nu} + \tilde{T}_{\mu\nu}, \quad (9)$$

where $\tilde{T}_{\mu\nu}$ contains the regular part and η is a function of the coordinates which vanishes on the junction surface, is non-zero everywhere else, and on the junction surface its gradient is a unit vector. The tensor $S_{\mu\nu}$ is called the surface stress-energy (or energy-momentum) tensor. The δ -function restricts its influence to the junction surface and we assume that it only depends on coordinates on the junction surface, *i.e.*, in our case this tensor does not depend on R . The Lanczos equation [5] relates the surface energy-momentum tensor $S_{\mu\nu}$ to the jump in the extrinsic curvature $K_{\mu\nu}$ of the junction surface by

$$\kappa S^{\mu\nu} = {}^{(3)}g^{\mu\nu} [K] - [K^{\mu\nu}], \quad (10)$$

or equivalently (after taking the trace and substituting back for K)

$$\frac{1}{\kappa} [K^{\mu\nu}] = -S^{\mu\nu} + \frac{1}{2} {}^{(3)}g^{\mu\nu} S, \quad (11)$$

where $K \stackrel{\text{def}}{=} K^\mu_\mu$, $S \stackrel{\text{def}}{=} S^\mu_\mu$, and $\kappa \stackrel{\text{def}}{=} 8\pi G$. These two equations imply that the presence of a surface layer is equivalent to a jump in the extrinsic curvature, *i.e.*, $\gamma^{\mu\nu} \stackrel{\text{def}}{=} [K^{\mu\nu}] \neq 0$.

To relate this conditions to the metric components on both sides of the junction surface we have to find expressions for the extrinsic curvature. We start with the normal to the junction surface, which is given by

$$n_\mu = \delta_\mu^R \frac{l\alpha}{\sqrt{1 - R^2 \dot{\alpha}^2 l^2}} \Big|_{R=1}, \quad (12)$$

and the unique timelike unit-vector tangential to the junction surface and orthogonal to the spherical symmetric subspace, which is given by

$$u^\mu = \frac{1}{k} \delta_t^\mu. \quad (13)$$

The extrinsic curvature $K_{\mu\nu} = n_{(\lambda;\kappa)} h^\lambda_\mu h^\kappa_\nu$, where $h^{\mu\nu} = g^{\mu\nu} - n^\mu n^\nu$ is the projection tensor onto the junction surface, has the two independent components

$$K_{\mu\nu} u^\mu u^\nu = \frac{1}{k^3 N l \alpha} \Gamma_{Rtt} = -\frac{\dot{N} + 2N' l \dot{\alpha} + \dot{\alpha}^2 l^2 N (\dot{l}/l)}{k^3 \dot{\alpha} l}. \quad (14)$$

$$K^\theta_\theta = \frac{N}{k w} (\dot{\alpha} l (l f)^\bullet + (l f)'), \quad (15)$$

where we used the coordinate time derivative of (7) to simplify the first expression.

This form of the extrinsic curvature implies that the surface energy-momentum tensor $S^{\mu\nu}$ is diagonal and of perfect-fluid form (in the three-dimensional hypersurface space). We introduce the surface energy density ρ_s and pressure p_s such that

$$S^{\mu\nu} = (\rho_s + p_s) u^\mu u^\nu + p_s {}^{(3)}g^{\mu\nu}. \quad (16)$$

The Lanczos equations (11) are now given by the two equations

$$[N\{\dot{\alpha} l (l f)^\bullet + (l f)'\}] = -\frac{\kappa}{2} \rho_s w k \quad (17)$$

$$[\dot{N} + 2N' l \dot{\alpha} + \dot{\alpha}^2 l^2 N (\dot{l}/l)] = \kappa \left(\frac{1}{2} \rho_s + p_s \right) k^3. \quad (18)$$

The Gauss-Codazzi equations relate the curvature at one point to the extrinsic and intrinsic curvature of a hypersurface which passes through this point by

$$R_{\mu\nu\lambda\kappa} e_a^\mu e_b^\nu e_c^\lambda e_d^\kappa = {}^{(3)}R_{abcd} + \epsilon (K_{ad} K_{bc} - K_{ac} K_{bd})$$

and $R_{\mu\nu\lambda\kappa} n^\mu e_b^\nu e_c^\lambda e_d^\kappa = K_{bc|d} - K_{bd|c}$, where e_a^μ is a coordinate basis of the junction surface, a vertical bar denotes the covariant derivative with respect to the induced hypersurface metric $h_{\mu\nu} = g_{\mu\nu} - n_\mu n_\nu$, and $\epsilon \stackrel{\text{def}}{=} n^\mu n_\mu$ equals $+1$ for timelike hypersurfaces, and -1 for spacelike hypersurfaces. For a timelike hypersurface these equations lead to [13] (after substituting (11))

$$[G_{\mu\nu} e_a^\mu n^\nu] = -\kappa S_a^b |_b \quad (19)$$

$$[G_{\mu\nu} n^\mu n^\nu] = \frac{1}{2} [K^2 - K_{\mu\nu} K^{\mu\nu}] = \kappa S^{\mu\nu} \bar{K}_{\mu\nu}, \quad (20)$$

where $\bar{K}_{\mu\nu} \stackrel{\text{def}}{=} \frac{1}{2} (\lim_{R \rightarrow 1+} K_{\mu\nu} + \lim_{R \rightarrow 1-} K_{\mu\nu})$ and $G_{\mu\nu} \stackrel{\text{def}}{=} R_{\mu\nu} - \frac{1}{2} g_{\mu\nu} R$ is the Einstein tensor.

The second of these equations represents nothing else than the definition of the surface stress-energy tensor $S^{\mu\nu}$ (which was substituted) and hence is redundant. Using (16) to evaluate (19) we find that the only non-vanishing component is the time component, which is given by (using $e_0^\mu = u^\mu$)

$$k u^\mu \rho_{s;\mu} + k (\rho_s + p_s) u^a |_a = \kappa^{-1} [G_{\mu\nu} u^\mu n^\nu] = [T_{\mu\nu} u^\mu n^\nu], \quad (21)$$

where the last equality follows from the Einstein equation and $u^a |_a = u^\mu (2 \ln(l f))_{;\mu}$. Together with an equation of state for the surface energy and pressure densities this equation describes the evolution of the ‘matter’ on the surface.

2.4 Matching with surface-layer

The second geometric matching condition shows that $k \stackrel{\text{def}}{=} N \sqrt{1 - \dot{\alpha}^2 l^2}$ is continuous across the junction surface. Hence we can express the junction surface motion in terms of the lapse function by

$$\dot{\alpha} l = \pm \sqrt{1 - \left(\frac{k}{N} \right)^2}. \quad (22)$$

For convenience we will choose now $k = 1$, i.e., the coordinate time corresponds to proper time along the curves $R = 1, \theta, \phi$ constant on the junction surface. Setting $u \stackrel{\text{def}}{=} N/k$ and $j_{\pm} \stackrel{\text{def}}{=} \text{sgn}(\dot{\alpha}_{\pm})$ the angular component of the extrinsic curvature (15) on both sides of the junction surface and equation (8), the derivative of the junction surface radius with respect to coordinate time, are given by

$$K^{\theta}_{\theta} = (uw' + j\dot{w}\sqrt{u^2 - 1})/w \quad (23)$$

$$L \stackrel{\text{def}}{=} \frac{dw}{dt} = uw + jw'\sqrt{u^2 - 1} \quad (24)$$

A valid matching between two spherically symmetric sections, each satisfying the Einstein-field equations, must satisfy the two geometric matching conditions ((3) and (4)) and the two independent components of the Lanczos equation ((17) and (18)). We first note, that if the first geometric matching condition (matching of the surface radius) (3) is satisfied initially, then it is sufficient to demand that its coordinate time derivative (8) is satisfied at all times. Secondly, with our choice of variables the second geometric matching condition (4) is nothing more than an identity — with (22) it has already been used to eliminate one variable. Thirdly, as will be shown in section 4, equation (18), the time-component of the Lanczos equation, is in fact identically satisfied if all the other matching conditions are satisfied, the Einstein-field equations are valid on each side, and the surface-matter evolution is given by (21).

We conclude that the matching conditions are completely represented by (8), the coordinate time derivative of the first geometric matching condition, and the angular component of the Lanczos equation (17) together with an initial matching of the proper surface radius $w = lf$. With our choice of variables these equations take the (surprisingly symmetric) form

$$[L] = [u\dot{w} + jw'\sqrt{u^2 - 1}] = 0 \quad (25)$$

$$[wK^{\theta}_{\theta}] = [uw' + j\dot{w}\sqrt{u^2 - 1}] = -E, \quad (26)$$

where $w \stackrel{\text{def}}{=} lf$ is the proper surface radius of the spherical junction surface on each side and

$$E \stackrel{\text{def}}{=} \frac{\kappa\rho_s w}{2} \quad (27)$$

quantifies the energy-content of the layer. To find a relation between K^{θ}_{θ} and L we square (23) and substitute L^2 from the square of (24) and obtain

$$(wK^{\theta}_{\theta})^2 = L^2 + a, \quad (28)$$

where $a \stackrel{\text{def}}{=} w'^2 - \dot{w}^2$. Versions of this equation have been given in [9] and [12]. For $E \neq 0$ we can express K^{θ}_{θ} in terms of L by using an algebraic identity as

$$wK^{\theta}_{\theta} = \frac{[(wK^{\theta}_{\theta})^2] \pm [wK^{\theta}_{\theta}]^2}{2[wK^{\theta}_{\theta}]} = \frac{b \pm E^2}{-2E}, \quad (29)$$

where $b \stackrel{\text{def}}{=} a_+ - a_-$. The explicit expression for L in terms of E takes the form

$$L^2 = \left(\frac{b - E^2}{2E}\right)^2 - a_- = \left(\frac{b + E^2}{2E}\right)^2 - a_+ = (E^4 - 2E^2(a_+ + a_-) + b^2)/4E^2, \quad (30)$$

Note that we find by differentiating (23) and (24) with respect to u (taking w, \dot{w} , and w' to be independent of u) the helpful relations

$$j\sqrt{u^2 - 1}\frac{\partial L}{\partial u} = wK^{\theta}_{\theta} \quad \text{and} \quad j\sqrt{u^2 - 1}\frac{\partial wK^{\theta}_{\theta}}{\partial u} = L, \quad (31)$$

which are valid on each side of the junction surface.

The geometric matching condition (24) can be solved for u_{\pm} and j_{\pm} in terms of the time derivative of the surface radius L and the extrinsic curvature component K^{θ}_{θ}

$$u = \frac{\dot{w}L - w'wK^{\theta}_{\theta}}{-a}. \quad (32)$$

We note that differentiating (32) with respect to u and using (31) yields

$$j\sqrt{u^2 - 1} = \frac{w'L - \dot{w}wK^{\theta}_{\theta}}{a}, \quad (33)$$

what also determines the sign of j and hence the radial direction of motion of the junction surface for each side.

2.5 The ‘no surface-layer’ case

If all tangential components of the extrinsic curvature are continuous at the junction surface then it follows from (26) that the surface-energy density ρ_s vanishes. In this case the junction hypersurface is called a boundary-surface. It is an immediate consequence of (28) that

$$E = \frac{\kappa \rho_s w}{2} = 0 \Rightarrow b = [a] = [w'^2 - \dot{w}^2] = 0,$$

and $b = 0 \Rightarrow E = 0$ or $E = wK_{-\theta}^\theta/2 = -wK_{+\theta}^\theta/2$.

Feasible solutions need to satisfy the two geometric matching conditions (3) and (4), the derivative of the first matching condition (8) and the matching of the extrinsic curvature (17). Recognizing the similar structure of (8) and (17) we form two new equivalent equations by adding and subtracting the two equations. The result reads

$$[N(1 - \dot{\alpha}l)(w' - \dot{w})] = 0 \quad [N(1 + \dot{\alpha}l)(w' + \dot{w})] = 0.$$

Using the factorized form of the second geometric matching condition (4) and defining $q = N(1 - \dot{\alpha}l)$ this becomes

$$[q(w' - \dot{w})] = 0 \quad \left[\frac{1}{q}(w' + \dot{w})\right] = 0. \quad (34)$$

If both $w' - \dot{w}$ and $w' + \dot{w}$ vanish separately on both sides, then the system becomes an identity and the junction surface motion remains undefined. Let us assume now that this is not the case.

We note that for $[w'] = [\dot{w}] = 0$ the system is solved for any $q_+ = q_-$. Hence, if the angular component of the metric and its first order proper time and radial derivatives are continuous, then the junction surface motion does not follow from the matching conditions. In particular, this is the case for the trivial matching of two identical space-times, were we have an ‘imaginary junction surface’, which could be placed anywhere.

Let us from now on assume that at least one of the proper derivatives of w is not continuous at the junction surface.

If $w' \pm \dot{w}$ is zero on one side, it has to be zero on the other side too (otherwise no matching is possible) and one of the equations (34) is identically satisfied.

However, if all $w'_\pm \pm \dot{w}_\pm$ are non-zero then the condition $b = 0$ also guarantees that the two linear equations (34) are linearly dependent. The motion of the boundary surface is then described by the four equations (if $w' \pm \dot{w}$ is zero then one of the options in the first equation is undefined, but the other option is then still valid)

$$\frac{N_+(1 - \dot{\alpha}_+^2 l_+^2)}{N_-(1 - \dot{\alpha}_-^2 l_-^2)} = \frac{w'_- - \dot{w}_-}{w'_+ - \dot{w}_+} = \frac{w'_+ + \dot{w}_+}{w'_- + \dot{w}_-} \quad N_\pm^2(1 - \dot{\alpha}_\pm^2 l_\pm^2) = 1 \quad \frac{db}{dt} = 0, \quad (35)$$

where

$$\frac{db}{dt} = 2[Nw' \{(w')^\bullet + w''\dot{\alpha}l\} - \dot{w}N\{\ddot{w} + (\dot{w})'\dot{\alpha}l\}]. \quad (36)$$

2.6 Expansion for small surface-energy densities

As will be seen in the numerical examples given later, in many cases the surface-energy density (and hence E) approaches zero at some finite coordinate time. In the case of $b \neq 0$ the dynamic quantities can be approximated by a series expansion in terms of E . We start by re-writing the exact expression for the extrinsic curvature (29) as

$$wK_{\pm\theta}^\theta = -\frac{b}{2E} \mp \frac{E}{2}.$$

It follows then from (30) that

$$\pm L = \frac{|b|}{2E} - \frac{a_+ + a_-}{2|b|}E + O(E^3),$$

where $O(E^3)$ represents terms of the order E^3 or smaller. Furthermore, from (32) we find for $u = N/k$ the expansion

$$u_\pm = -\frac{w'_\pm b + \text{sgn}(L)\dot{w}_\pm|b|}{2a_\pm} \frac{1}{E} + \frac{\text{sgn}(L)\dot{w}_\pm(a_+ + a_-)/|b| \mp w'_\pm}{2a_\pm} E + O(E^3).$$

As the surface-energy density approaches zero the lapse functions (given by u_+ and u_-) diverge and the proper speed of the junction surface approaches the speed of light quadratically since

$$|\dot{\alpha}_\pm l_\pm| = 1 - \frac{2\alpha_\pm l_\pm^2}{w'_\pm b + \text{sgn}(L)\dot{w}_\pm|b|} E^2 + O(E^4).$$

To examine if and how E approaches zero we finally expand the evolution equation (21)

$$\frac{dE}{dt} = \frac{\kappa}{2} \left(w[T_{\mu\nu}u^\mu n^\nu] - \frac{|b|}{w} \left(\gamma_s - \frac{1}{2} \right) \right) + O(E^2).$$

Generally the first term diverges as we approach the speed of light — for example in the case of a perfect fluid one finds

$$|T_{\mu\nu}u^\mu n^\nu| = \left(\frac{w'b + \text{sgn}(L)\dot{w}|b|}{2a} \right)^2 (\rho + p) \frac{1}{E^2} + O(E^0).$$

We conclude that if the energy-momentum contribution $[T_{\mu\nu}u^\mu n^\nu]$ has a sign opposite to E , then E accelerates towards zero. In many cases E will reach zero at some finite coordinate time t_0 . Close to this point and assuming that the time dependence of all other terms is negligible we have $E \propto (t_0 - t)^{1/3}$. This implies that the lapse functions are integrable and the junction surface reaches the speed of light (on each side) within a finite proper time. Here our formalism breaks down and one would need a separate treatment of these singular cases. We want to speculate here that at these points the junction surface turns spacelike.

On the other hand, if the sign of $[T_{\mu\nu}u^\mu n^\nu]$ is the same as the sign of E then E cannot get arbitrarily close to zero. In some cases (see figure 7) E will oscillate around some value (which is itself time dependent). Even in these cases we can encounter divergencies resulting from diverging a_\pm and b . This can lead to non-integrable lapse functions - from each side the junction seems to exist forever, but an observer who moves along the junction encounters a singular point after a finite time. At this point the surface energy density is zero and again the formalism breaks down.

It should be noted that in the case of a perfect fluid on both sides of the junction the sign of the stress-energy contribution $[T_{\mu\nu}u^\mu n^\nu]$ depends on the energy density ρ and pressure p on both sides, i.e., on the equations of state. Hence whether a particular junction reaches the speed of light within a finite time or not might depend on the equation of state on each side. In section 6 we give a numerical example for such a case.

Because points on the junction surface are not causally connected a spacelike junction surface has a very different physical interpretation . In such cases the junction surface cannot be treated as an ‘evolving system’ on its own, but rather as some kind of (spacelike) transition surface which is generated by the physics underlying the cosmological model.

Usually a timelike junction surface is used to model the time evolution of a spatially *localized* inhomogeneity. If a junction surface turns spacelike a breakdown in the thin wall approximation must have occurred.

3 Necessary and sufficient conditions for a possible matching

3.1 Demanding real solutions for L

From (30) we find with $L^2 \geq 0$ a necessary condition for the existence of solutions which restricts the allowed values for E , such that

$$E^4 - 2E^2(a_+ + a_-) + b^2 \geq 0. \quad (37)$$

The roots of the quadratic polynomial (in E^2) on the left-hand side are given by $a_+ + a_- \pm 2\sqrt{a_+ a_-}$. For $a_+ a_- < 0$ or $a_+ < 0, a_- < 0$ all values of E are feasible. Hence it is only for $a_+ \geq 0, a_- \geq 0$ that restrictions on E arise, which take the form

$$0 \leq |E| \leq |\sqrt{a_+} - \sqrt{a_-}| \quad \text{or} \quad \sqrt{a_+} + \sqrt{a_-} \leq |E|. \quad (38)$$

The shape of the forbidden region takes a particular simple form in the $E - \frac{b}{E}$ plane, which is illustrated in figure 2.

The two disjoint regions allowed for $|E|$ given by (38) are easily distinguished by $E^2 \leq |b|$ and $E^2 \geq |b|$. Furthermore, from (29) we find $\text{sgn}(K_{-\theta}^\theta) = \text{sgn}(K_{+\theta}^\theta) = -\text{sgn}(b/E)$ for $E^2 < |b|$ and $\text{sgn}(K_{-\theta}^\theta) = \text{sgn}(E), \text{sgn}(K_{+\theta}^\theta) = -\text{sgn}(E)$ for $E^2 > |b|$.

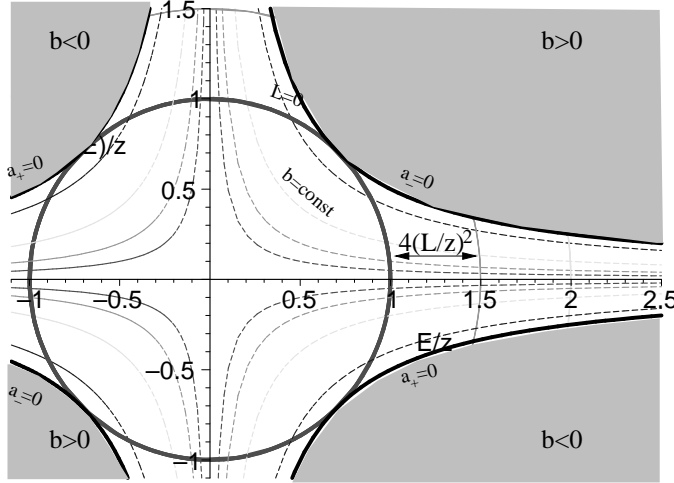


Figure 2: For the case $a_+, a_- \geq 0$ this figure shows the region in the $\frac{E}{z} - \frac{b}{Ez}$ -plane with $z \stackrel{\text{def}}{=} \sqrt{2(a_+ + a_-)}$ where there is no solution for the junction surface motion. The dashed lines show the curves of constant b , the circles are the lines of constant L/z , and the shaded region is not feasible since by construction $2|b| \leq z^2$.

3.2 Proper time relations

By setting $k = 1$ it follows from (5) the condition

$$N = u \geq +1, \quad (39)$$

i.e., on each side of the junction surface proper time must proceed faster (with respect to the time coordinate) than on the junction surface. To investigate the resulting constraints on the surface energy density we start by noting that

$$|w'(wK^\theta_\theta) - a| - |\dot{w}L| \begin{cases} \geq 0 & \text{for } a \geq 0 \\ \leq 0 & \text{for } a \leq 0 \end{cases}, \quad (40)$$

which can be easily verified by squaring and substituting from (28). Substituting (32) the inequality (39) takes the form

$$\frac{(w'(wK^\theta_\theta) - a) - \dot{w}L}{a} \geq 0.$$

It follows from (40) that for $a > 0$ we need $w'(wK^\theta_\theta) - a \geq 0$, while for $a < 0$

$$\dot{w}L \geq 0. \quad (41)$$

Let us first consider the case $a > 0$. Using (29) the condition becomes $w'(b + \sigma E^2)/(-2E) - a \geq 0$, where $\sigma = \pm 1$ corresponding to the outside (+) and inside (-) case. In the following let us use the convention that if a, w refer to the quantities on one side, then a_*, w_* refer to the quantities on the other side of the junction. By setting $x \stackrel{\text{def}}{=} \text{sgn}(b)E/\sqrt{|b|}$, $\epsilon_\pm \stackrel{\text{def}}{=} \pm \text{sgn}(b) = \text{sgn}(a - a_*)$, and $s_\pm \stackrel{\text{def}}{=} -\frac{a_\pm}{w'_\pm \sqrt{|b|}}$ we bring the inequality in the form

$$\frac{1}{x} + \epsilon_\pm x \begin{cases} \leq 2s_\pm & \text{for } w'_\pm > 0 \\ \geq 2s_\pm & \text{for } w'_\pm < 0 \end{cases}. \quad (42)$$

The allowed ranges for x are illustrated in figure 3.

The case of $\epsilon > 0$ Let us note that if $\epsilon_+ > 0$ then $\epsilon_- < 0$ and vice versa ($\epsilon_* < 0$). The sign of the surface energy density is now determined by

$$\text{sgn}(\rho_s) = -\text{sgn}(b)\text{sgn}(w'). \quad (43)$$

Furthermore, if $|s| = |a/(w'\sqrt{|b|})| \leq 1$ then no restrictions are placed on $|x|$ (but further restrictions could come from $a_* > 0$). For $|s| > 1$ the allowed range can be found by setting $|x| = e^z$ and hence $|1/x + x| = 2 \cosh(z)$. Using $\cosh^{-1}|s| = \ln(|s| + \sqrt{s^2 - 1})$ one obtains the ranges

$$0 < |x| \leq |s| - \sqrt{s^2 - 1} \quad \text{or} \quad |s| + \sqrt{s^2 - 1} \leq |x|.$$

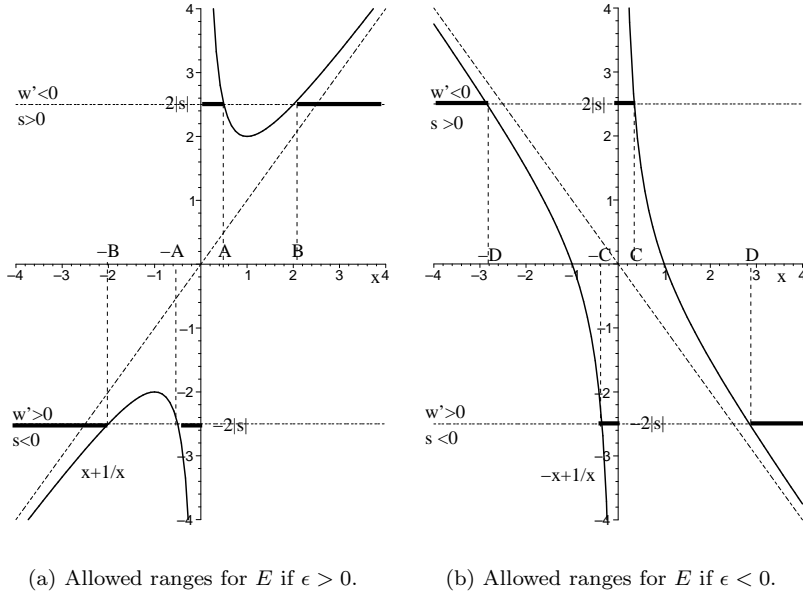


Figure 3: Visualization of the inequality (42) for $\epsilon > 0$ (figure 3(a)) and $\epsilon < 0$ (figure 3(b)). The lower and upper horizontal line correspond to $w'_\pm > 0$ and $w'_\pm < 0$, respectively. Here $s_\pm \stackrel{\text{def}}{=} -a_\pm/(w'_\pm \sqrt{|b|})$ are the terms on the right-hand side of (42). The allowed ranges are indicated by a bold line. The end-points are given by (A and B are only defined for $|s| > 1$) $A = |s| - \sqrt{s^2 - 1}$, $B = |s| + \sqrt{s^2 - 1}$, $C = -|s| + \sqrt{s^2 + 1}$, $D = |s| + \sqrt{s^2 + 1}$.

The case of $\epsilon < 0$ Similarly to the last case, if $\epsilon < 0$ then $\epsilon_* > 0$. Hence each case will occur once at the junction. A similar procedure as above yields the restrictions

$$|s| - \sqrt{s^2 + 1} \leq \text{sgn}(w')x < 0 \quad \text{or} \quad |s| + \sqrt{s^2 + 1} \leq \text{sgn}(w')x.$$

The case of $a > 0$ on both sides If a is positive on both sides then x can only take values which lay in the intersection of the allowed ranges on each side. The allowed intervals differ, depending on the signs of w'_+ and w'_- . All possible cases are shown in table 1. We note that in every case the allowed values for E have the same sign.

As a particularly important case (for the matching of FLRW models) and an illustrative example we evaluate the restrictions on the surface energy density for $a_+, a_- > 0$ and $w'_+, w'_- > 0$. In this case x has to be negative and hence $\text{sgn}(\rho_s) = \text{sgn}(E) = -\text{sgn}(b)$. If one assumes on physical grounds that ρ_s should be positive then no matching will be possible if b is positive.

The case of $a < 0$ If $a < 0$ on one side of the junction surface then (41) implies with $\text{sgn}(L) = \text{sgn}(\dot{w})$ the sign for L , the coordinate time derivative of the surface radius, which was left undefined in (30). For the case that a_+ and a_- are negative this condition must hold on both sides and hence a matching is only possible if

$$\text{sgn}(\dot{w}_+) = \text{sgn}(\dot{w}_-) \quad \text{for } a_+, a_- < 0. \quad (44)$$

4 The time-component of the Lanczos equation

So far we have only considered matching of the metric and of the angular components of the extrinsic curvature of the junction surface. The remaining matching condition comes from the time-component of the extrinsic curvature (18), which contains a second order time derivative of the junction coordinate radius, or equivalently a first-order time derivative of the lapse function.

	$b > 0$ $\Rightarrow \epsilon_+ = +1, \epsilon_- = -1$ $\text{sgn}(\rho_s) = -1$	$b < 0$ $\Rightarrow \epsilon_+ = -1, \epsilon_- = +1$ $\text{sgn}(\rho_s) = +1$
$w'_+ > 0$ $w'_- > 0$	$\sqrt{ b } \max(-A_+, -C_-) \leq E < 0$ for $ s_+ > 1$ $-\sqrt{ b }C_- \leq E < 0$ for $ s_+ \leq 1$ $\text{sgn}(\rho_s) = -1$	$0 < E \leq \sqrt{ b } \min(A_-, C_+)$ for $ s_- > 1$ $0 < E \leq \sqrt{ b }C_+$ for $ s_- \leq 1$ $\text{sgn}(\rho_s) = -1$
$w'_+ > 0$ $w'_- < 0$	$E \leq \sqrt{ b } \min(-B_+, -D_-)$ for $ s_+ > 1$ $E \leq -\sqrt{ b }D_-$ for $ s_+ \leq 1$ $\text{sgn}(\rho_s) = -1$	$E \leq \sqrt{ b } \min(-B_-, -D_+)$ for $ s_- > 1$ $E \leq -\sqrt{ b }D_+$ for $ s_- \leq 1$ $\text{sgn}(\rho_s) = -1$
$w'_+ < 0$ $w'_- > 0$	$\sqrt{ b } \max(B_+, D_-) \leq E$ for $ s_+ > 1$ $\sqrt{ b }D_- \leq E$ for $ s_+ \leq 1$ $\text{sgn}(\rho_s) = +1$	$\sqrt{ b } \max(B_-, D_+) \leq E$ for $ s_- > 1$ $\sqrt{ b }D_+ \leq E$ for $ s_- \leq 1$ $\text{sgn}(\rho_s) = +1$
$w'_+ < 0$ $w'_- < 0$	$0 < E \leq \sqrt{ b } \min(A_+, C_-)$ for $ s_+ > 1$ $0 < E \leq \sqrt{ b }C_-$ for $ s_+ \leq 1$ $\text{sgn}(\rho_s) = +1$	$\sqrt{ b } \max(-A_-, -C_+) \leq E < 0$ for $ s_- > 1$ $-\sqrt{ b }C_+ \leq E < 0$ for $ s_- \leq 1$ $\text{sgn}(\rho_s) = -1$

Table 1: For $a_+ > 0$ and $a_- > 0$ this table shows the allowed region for E for all possible combinations of $\text{sgn}(w'_+)$ and $\text{sgn}(w'_-)$. Here $A_{\pm} = |s_{\pm}| - \sqrt{s_{\pm}^2 - 1} \leq 1$; $B_{\pm} = |s_{\pm}| + \sqrt{s_{\pm}^2 - 1} \geq 1$; $C_{\pm} = -|s_{\pm}| + \sqrt{s_{\pm}^2 + 1} \leq 1$; $D_{\pm} = |s_{\pm}| + \sqrt{s_{\pm}^2 + 1} \geq 1$. and $s_{\pm} = -a_{\pm}/(w'_{\pm} \sqrt{|b|})$.

Rewriting the time-component of the extrinsic curvature in terms of our variable $u = N/k$ yields

$$-K^{\mu\nu}u_{\mu}u_{\nu} = \frac{j}{\sqrt{u^2 - 1}} \frac{du}{dt} + j\sqrt{u^2 - 1} \frac{i}{l} + u \frac{N'}{N}, \quad (45)$$

where the factor N'/N is independent of the junction surface motion. Taking the coordinate time derivative of (29) and using (23) and (31) we obtain

$$\frac{j_{\pm}L}{\sqrt{u_{\pm}^2 - 1}} \frac{du_{\pm}}{dt} = -\frac{1}{2E} \frac{db}{dt} - \frac{dE}{dt} \frac{1}{E} w K_{\mp\theta}^{\theta} - z, \quad (46)$$

where (note that $(d/dt)f(t, \alpha(t)R) = u\dot{f} + j\sqrt{u^2 - 1}f'$)

$$z \stackrel{\text{def}}{=} u \frac{dw'}{dt} + j\sqrt{u^2 - 1} \frac{d\dot{w}}{dt} = ju\sqrt{u^2 - 1}\{w'' + \ddot{w}\} + u^2(w')^{\bullet} + (u^2 - 1)(\dot{w}).$$

Differentiating (27) and using (21) with $u^a|_a = 2L/w$ yields

$$\frac{dE}{dt} = -\kappa L \left(\frac{\rho_s}{2} + p_s \right) + \kappa \frac{w}{2} [T_{\mu\nu}u^{\mu}n^{\nu}],$$

which expresses the coordinate time derivative of E . Substituting for the first term in (45) allows us to evaluate the remaining junction condition $[K^{\mu\nu}u_{\mu}u_{\nu}] = -\kappa(\rho_s/2 + p_s)$. The terms containing the surface pressure and density cancel each other and we obtain

$$0 = \frac{\kappa}{2} w [T^{\mu\nu}u_{\mu}n_{\nu}] + [z] - L \left[j\sqrt{u^2 - 1} \frac{i}{l} \right] - L \left[u \frac{N'}{N} \right]. \quad (47)$$

The first term can be expressed in terms of the Einstein-tensor with respect to the original metric (1) as

$$\kappa T_{\mu\nu}u^{\mu}n^{\nu} = G_{\mu\nu}u^{\mu}n^{\nu} = ju\sqrt{u^2 - 1} \left(\frac{G_{tt}}{N^2} + \frac{G_{rr}}{l^2} \right) + (2u^2 - 1) \left(\frac{G_{tr}}{Nl} \right),$$

where the relevant components of the Einstein-tensor are given by

$$\begin{aligned} G_{tt} &= \frac{2N^2}{w} \left(-w'' + \dot{w} \frac{i}{l} + \frac{1-a}{2w} \right) \\ G_{rr} &= \frac{2l^2}{w} \left(\ddot{w} - w' \frac{N'}{N} + \frac{1-a}{2w} \right) \\ G_{tr} &= \frac{2Nl}{w} \left(\dot{w} \frac{N'}{N} - (w')^{\bullet} \right), \end{aligned}$$

and L is given by (24). Substituting into (47) and using the relation

$$(\dot{w})' - (w')^\bullet = \frac{\dot{l}}{l}w' - \frac{N'}{N}\dot{w}$$

shows that (47) is an identity, satisfied for all spherically symmetric junctions between solutions of the Einstein-field equations if the geometric matching conditions ((3) and (4)) together with the angular component of the Lanczos equation (26) are satisfied. While it was well-known that for certain cases the time-component of the Lanczos equation is identically satisfied (e.g. [8, 11]), it seems to be a new result for the generic spherically symmetric case.

It was suggested that for the matching of FLRW models the time-component of the Lanczos equation determines the pressure [9]. In light of the above result this cannot be the case and one needs to supplement the model with an equation of state for the surface-matter.

5 Matching of FLRW sections

We want to turn our attention now to the special case of the matching of two distinct FLRW regions. Such junctions are encountered in cosmological models which approximate universes containing many FLRW domains (multidomain universes). The most prominent example is Linde's Chaotic Inflation scenario [3, 4].

Junctions of this type have been studied in [9, 12]. Our treatment will serve as an illustration for the introduced method and as a source for numerical examples. Here it is not our aim to investigate physical processes which could lead to creation of a "bubble" and we refer the interested reader to the vast literature (see, e.g., [9, 14, 15, 16, 17]). Instead we want to focus on the generic geometrical and mathematical aspects.

5.1 FLRW models and their parametrization

The metric of FLRW models can be written in the form

$$ds^2 = -N^2(t)dt^2 + l^2(t)\{dr^2 + f^2(r)d\Omega^2\}, \quad (48)$$

where $l(t)$ is the scale factor, $N(t)$ the so-called lapse function, $d\Omega$ the line-element on the two-dimensional unit-sphere, and

$$f(r) = \begin{cases} \sin(r) & \text{for closed models} \\ r & \text{for flat models} \\ \sinh(r) & \text{for open models} \end{cases}.$$

Note that the FLRW metric (48) has the same form as the general metric for spherical symmetric spaces (1), but with $l' = 0$, $N'/N = 0$ and $\dot{f} = 0$.

The evolution of FLRW models is described by the Friedmann equation - the dynamic part of the Einstein-Field equations -

$$\left(\frac{\dot{l}}{l}\right)^2 - \frac{\kappa\rho + \Lambda}{3} = -\frac{\zeta}{l^2}, \quad (49)$$

where $\zeta = 0, +1, -1$ for flat, closed, and open models, respectively, and a dot indicates the derivative with respect to *proper* time t , i.e., $\dot{l} \stackrel{\text{def}}{=} \frac{1}{N}\frac{dl}{dt}$. The matter is described by an energy-momentum tensor of perfect fluid type. The unit tangent vectors to the fluid flow lines are given by²

$$v^\mu = \frac{1}{N}\delta_t^\mu,$$

and the energy-momentum tensor describing the comoving perfect fluid takes the form $T^{\mu\nu} = (\rho + p)v^\mu v^\nu + pg^{\mu\nu}$, where ρ is the energy density and p the pressure. The matter evolution is then described by the energy-conservation equation $\dot{\rho} + (\rho + p)3H = 0$, where $H \stackrel{\text{def}}{=} \dot{l}/l$ is the Hubble parameter.

We restrict ourself to models with a γ -law equation of state, i.e., models in which energy density ρ and pressure p are related by³

$$p = (\gamma - 1)\rho \quad \gamma \in (2/3, 2].$$

²In the new coordinate system which is continuous at the junction the components take the form $v^\mu = \frac{1}{N}\delta_t^\mu - \frac{\dot{\alpha}R}{\alpha}\delta_R^\mu$.

³The case $\gamma = 0$ gives an effective cosmological constant. We can exclude this case here because the cosmological constant is included separately.

In this case $\chi_\gamma \stackrel{\text{def}}{=} \frac{\kappa}{3}\rho l^{3\gamma}$ is a constant of motion. This allows us to eliminate the energy density ρ from the Friedmann equation (49), so that the evolution of the scale factor l is described in terms of the constants of motion by

$$H^2 = \chi_\gamma l^{-3\gamma} + \frac{1}{3}\Lambda - \frac{\zeta}{l^2}. \quad (50)$$

Junctions are often used as models for transition regions between two almost-FLRW regions. Underlying is the assumption that an initially small transition region remains small.

5.2 Comoving junction surface

Let us first investigate whether there could be a comoving junction surface for two FLRW models with γ -equation of state. This case is uniquely identified by $\dot{\alpha}_\pm = 0$.

From the geometric matching condition (specialized to the FLRW metric) (3) we find

$$l_+ = \underbrace{\frac{f_-(\alpha_-)}{f_+(\alpha_+)}}_{\text{const.}} l_-, \quad (51)$$

where the first factor is now time-independent.

Let us assume we are given a solution to the Friedmann equation with $\gamma = \gamma_-$, $\chi = \chi_-$, $\Lambda = \Lambda_-$, and $\zeta = \zeta_-$. The question is now, whether there are constants γ_+ , Λ_+ , χ_{γ_+} and ζ_+ such that $l_+ = \lambda l_-$ is a solution for constant $\lambda > 0$. Both solutions would have the same Hubble parameter $H \stackrel{\text{def}}{=} \frac{\dot{l}_+}{l_+} = \frac{\dot{l}_-}{l_-}$. Substituting in each case from the Friedmann equation (50) gives

$$\chi_{\gamma_-} l_-^{-3\gamma_-} + \frac{1}{3}\Lambda_- - \frac{\zeta_-}{l_-^2} = \chi_{\gamma_+} l_-^{-3\gamma_+} \lambda^{-3\gamma_+} + \frac{1}{3}\Lambda_+ - \frac{\zeta_+}{l_-^2} \frac{1}{\lambda^2},$$

which has to be satisfied for all values of l_- . On both sides all terms contain different powers of l (note that $-3\gamma \in (-2, 6]$). In order that both sides contain the same powers of l we need $\gamma_- = \gamma_+$. Comparing the coefficients gives then $\lambda = 1$, $\zeta_+ = \zeta_-$, $\Lambda_+ = \Lambda_-$, and $\chi_{\gamma_+} = \chi_{\gamma_-}$. Hence the solutions are identical.

We conclude that if the inside and outside of the bubble are evolving according to the Friedmann equation (49) with a γ -law equation of state then no non-trivial comoving junction is possible. We note that this result follows alone from the geometric matching condition (4) – it does not depend on the presence of a surface layer.

5.3 Matching of FLRW regions with surface-layer

The FLRW metric (48) implies $w = l(t)f(r)$ and by taking proper-time and radial derivatives we derive $\dot{w} = Hw$ and $w' = \frac{df}{dr}$. The component of the energy-momentum tensor which is needed to evaluate the surface-matter evolution according to (21) is easily found to be (for completeness we include k , which is set to unity)

$$[T^{\mu\nu}u_\mu n_\nu] = \left[\frac{N^2 \dot{\alpha} l(\rho + p)}{k^2} \right].$$

We proceed now by expressing all quantities related to the metric and its derivatives (a, b, w', \dot{w} etc.) in terms of FLRW model quantities. With $(df/dr)^2 = 1 - \zeta f^2$ we obtain the expressions $a \stackrel{(49)}{=} 1 - \frac{\kappa\rho + \Lambda}{3}w^2$.

First we want to examine which kind of bubbles could exist if there can only be a positive surface-energy density on the junction surface, i.e., $E > 0$. For reasonably small bubbles (such that the circumference increases with the radial coordinate) we have $a_+ > 0, a_- > 0$, and $w' > 0$. We find from table 1 that in this case

$$\text{sgn}(E) = -\text{sgn}(b) = \text{sgn}([\kappa\rho + \Lambda]),$$

and hence junctions are only possible if the inside FLRW region has a smaller total⁴ energy density than the outside region. This is illustrated in figure 5.3.

⁴The cosmological constant represents the vacuum energy density.

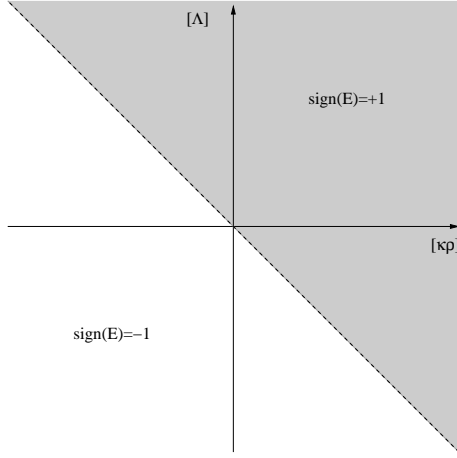


Figure 4: Points in the $\Lambda - \kappa\rho$ -plane for which a matching requires a positive/negative surface-energy density. Only certain matchings are possible if there can only be a positive surface energy density.

5.4 The closed to (inflating) open junction

To understand the behaviour of the junction surface it is instructive to consider a particularly simple example for which the evolution equations are known. One such example is the junction between a non-inflating closed geometry with radiation inside ($\Lambda_- = 0, \zeta_- = +1$) and an inflating empty open geometry outside ($\chi_+ = 0, \zeta_+ = -1$).

For these cases the Friedmann equation (50) is easily integrated and one finds the well-known solutions

$$l_-(\tau_-) = \sqrt{2\tau_- \chi_- - \tau_-^2} \quad l_+(\tau_+) = \sqrt{\frac{3}{\Lambda_+}} \sinh \left(\sqrt{\frac{\Lambda_+}{3}} \tau_+ \right), \quad (52)$$

where τ_+ and τ_- are the proper times along fluid flow-lines outside and inside, respectively. For the inside model the scale factor l_- grows until it reaches a maximum at $\tau_- = \chi_-$, and then declines until it reaches zero at $\tau_- = 2\chi_-$. On the contrary the outside model expands exponentially forever.

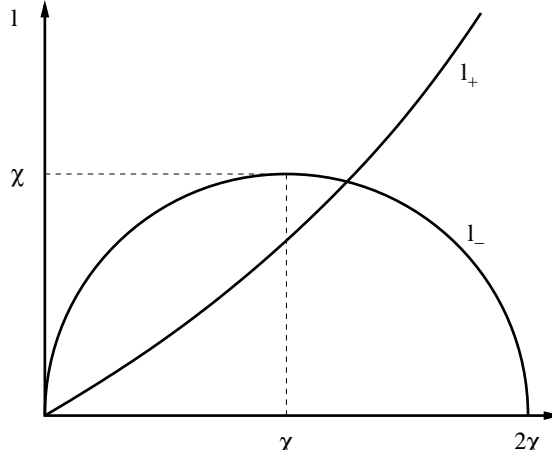


Figure 5: Evolution of the scale factor in a closed non-inflating FLRW model (l_-) and in an empty open inflating model (l_+).

Since for each time t the proper time measured along the junction surface is always less or equal to the proper time in the inside and outside model ($u_\pm \geq 1$) it is clear that such a boundary can only exist for a finite proper time measured along the junction — the (timelike) junction surface must be ‘terminated’ at some time.

There are four possible solutions. Firstly, it is possible that the junction surface exists forever (in terms of the proper time) in the outer region while the proper time along the junction surface is bounded. In our formalism this corresponds to a non-integrable divergence in the lapse function $N_+ = u_+$ for the outer region.

Secondly, the junction surface can contract to a point such that the inner region is eliminated. This case is characterized by α_+ , α_- and w approaching zero at some finite time.

Thirdly, the closed surface might detach from the open geometry — the birth of a child universe. In this case the radial coordinate for the closed geometry α_- approaches π , while α_+ and w vanish (see figure 6).

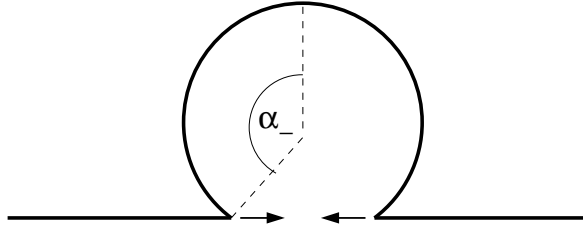


Figure 6: The closed inside geometry can detach from the open outside geometry. This happens when $\alpha_- \rightarrow \pi$ within a finite time.

As a last option the outside region might be eliminated. In the case of a closed outside geometry this is surely a possible solution, but in the cases of flat and open outside geometries this generally requires that the junction surface turns spacelike⁵.

In our formalism such a behaviour would yield a diverging, but integrable, lapse function. At the singularity we reach the speed of light and our formalism breaks down. Nevertheless, of the three options, to become super luminal, to continue at the speed of light, or to decelerate, the first one seems most convincing, also with view on the results of section 2.6.

Generally, one of these cases has to occur before we reach the singularity in the inside region as can be seen from the following argument. Let us assume that for physical reasons only positive surface energies are allowed. Since the outside geometry is open we have $w'_+ > 0$. As the closed inside geometry approaches the ‘big crunch’ singularity the energy density grows without bound. Hence $b = w^2(\kappa\rho_- - \Lambda_+)$ has to become positive at some stage during the contraction phase. However, from table 1 one can see that there is no solution possible with $w'_+ > 0$ and $b > 0$ if a_+ and a_- are positive. Let us note that when the inside region is contracting we have $\dot{w}_- < 0$ and $\dot{w}_+ > 0$. Hence according to (44) a_+ and a_- cannot be both negative. If a_+ is positive (and a_- negative) then (43) implies that the surface energy density is negative, which is in contradiction with our assumption. If on the other hand $a_+ < 0$ then this implies $L > 0$ and hence the proper surface radius would increase. This just helps driving $a_- = 1 - \kappa\rho_- w^2/3$ closer to zero, which eventually has to turn negative due to the diverging energy density. Again we reach a point where no solution is possible without negative surface energies.

Note that if one allows negative surface energies then the above argument shows that if the junction starts with a positive surface-energy density then at some point the junction must have a vanishing surface-energy density.

Figure 9 shows the results of a numerical integration of this particular model. It appears as if the speed of light is reached within a finite time (integrable lapse functions) on both sides. This strongly suggests to us that the junction turned spacelike. Note that this happens even far before the inner closed region enters the contracting phase.

With this example we want to emphasize that there are junctions which are possible initially, but which evolve to some singular point. Numerical studies have shown that this is rather common.

5.5 Vacuum bubbles

As a simple case vacuum bubbles ($\rho + p = 0$ on both sides) have frequently appeared in the literature [9, 12]. For these cases the surface energy-momentum tensor takes the form $S^\mu_\nu = -\rho_s \delta^\mu_\nu$ and it follows from (21) that ρ_s must be constant [9].

⁵One might speculate that for a closed inside geometry there has to be a finite volume and hence the junction surface has to turn backwards in time and become timelike again.

Assuming [12] $\kappa\rho + \Lambda = \text{const.}$ on each side one can integrate the evolution equation for the angular metric component (30) to obtain

$$w(t) = w_0 \cosh(t/w_0), \quad (53)$$

where t is the proper time along the junction and

$$w_0 = \frac{12\kappa\rho_s}{\sqrt{(4(\kappa(\rho_+ + \rho_-) + \Lambda_+ + \Lambda_-) + 3\kappa^2\rho_s^2)^2 - 64(\kappa\rho_+ + \Lambda_+)(\kappa\rho_- + \Lambda_-)}}, \quad (54)$$

which agrees with the findings in [12, 9].

However, this does not yet establish the actual motion of the junction surface since the relation of the proper time (along the junction) to the coordinate time is unknown — we need the lapse function which is given by (32). The proper time along fluid flow lines (which is proportional to coordinate time) is then given by $\int N dt$.

6 Numerical Results

A computer program has been written to integrate the evolution equations for several FLRW junctions numerically. To achieve better accuracy around the singularities a variable step-width was used. All examples given here are for positive surface-energy densities. Cases with negative surface energy can easily be constructed by exchanging the inside and outside region. The graphs on the following pages illustrate the results and will be discussed one-by-one below.

Open inside, inflating closed geometry outside Figure 7 shows such an example. After some time the surface radius starts to diverge (note the logarithmic scaling) while $E = \kappa w \rho_s / 2$ does not approach zero (hence close to the divergence $\rho_s \propto 1/w$). The proper times on both sides seem to be diverging, which is in agreement with the results from subsection 2.6. Note that the inner and outer regions have a rather unusual equation of state with $\gamma_+ = 0.7$ and $\gamma_- = 1.9$ — in this case it is really this choice of the equations of state which makes the energy-momentum tensor contribution $[T_{\mu\nu}u^\mu n^\nu]$ positive for small values of E (see subsection 2.6).

Figure 8 shows the evolution of the same initial situation, but with different equations of state (dust on both sides). This seems to change the sign of the energy-momentum contribution $[T_{\mu\nu}u^\mu n^\nu]$ for small values of E , which now approaches zero within a finite time. In fact, it can be verified that close to the singular point t_0 we have as expected $E \propto \sqrt[3]{t_0 - t}$. As predicted in subsection 2.6 the lapse functions appear to be integrable and the proper times do not diverge. The junction surface seems to reach the speed of light within a finite time.

Clearly, our formalism breaks down at this point. However, one could argue that after reaching the speed of light within a finite time, one should expect the junction to turn spacelike.

Closed inside, inflating open outside Figure 9 shows such a situation with a radiation equation of state for the inside region ($\gamma_- = 4/3$). This is the example discussed above.

7 Conclusion

We developed a formalism for the treatment of timelike junctions between spherically symmetric solutions of the Einstein-field equation, which is based on the Lanczos equation and the Israel junction conditions. We introduce new coordinates such that two conditions are satisfied: Firstly, all coordinates are continuous at the junction surface, and secondly, the junction surface becomes a surface of constant ‘radial’ coordinate. In this approach the actual movement of the junction surface is absorbed into the metric, of which the transverse components are discontinuous at the junction surface.

We evaluate the junction conditions and re-discover with (28) and (29) well-known relations between the extrinsic curvatures, the surface layer energy density, and the rate of change of the surface radius of the junction surface. It should be pointed out that these results follow without using the time-component of the Lanczos equation. As it was shown in section 4, for all spherically symmetric cases this remaining equation is in fact an identity. This was known for special cases, but it appears to be a new result in this general form.

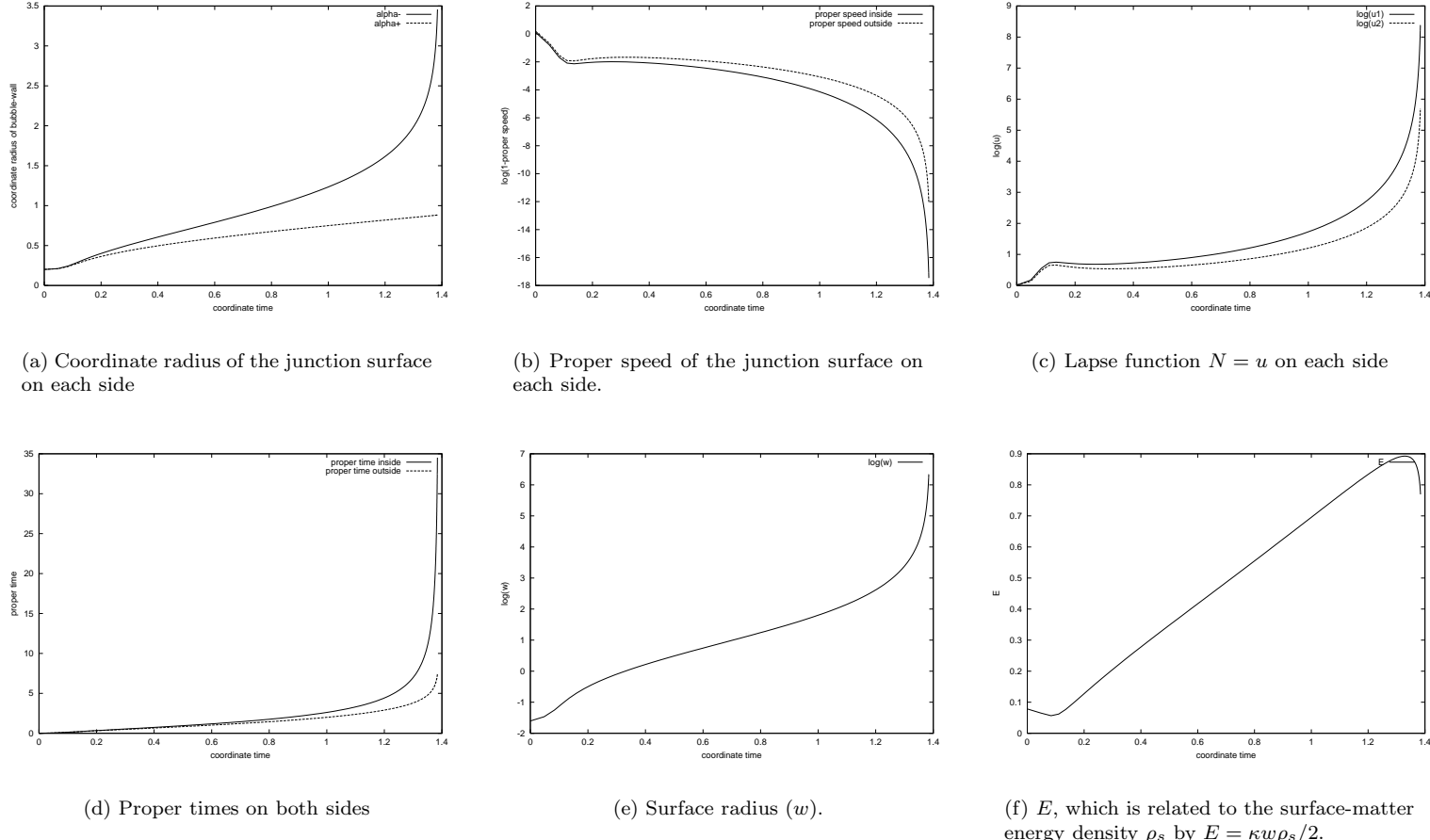


Figure 7: Evolution of a junction between an open (inside) and an inflating closed (outside) geometry. (Parameters: $\gamma_s = 1, \zeta_+ = +1, \zeta_- = -1, \chi_+ = 5, \chi_- = 2, \gamma_+ = 0.7, \gamma_- = 1.9, \Lambda_+ = 2, \Lambda_- = 0$; Initial values: $\rho_s = 0.031, \alpha_+ = 0.20272, \alpha_- = 0.2, l_+ = 1, l_- = 1, \rho_+ = 0.597, \rho_- = 0.239$.) Note that here u and w are plotted logarithmically.

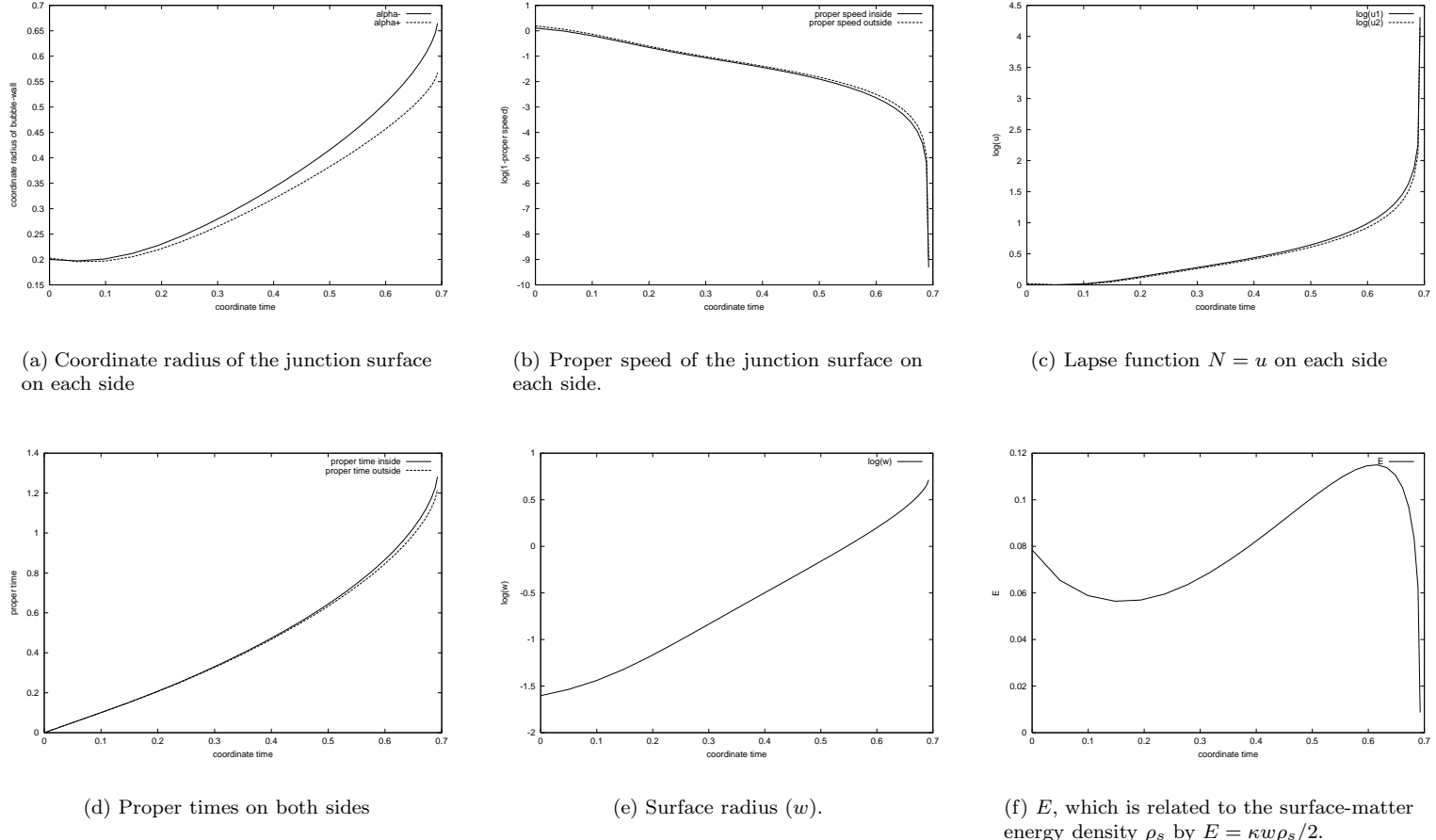


Figure 8: Evolution of a junction between an open (inside) and an inflating closed (outside) geometry. The lapse functions are integrable and the speed of light is reached within a finite time. (Parameters: $\gamma_s = 1, \zeta_+ = +1, \zeta_- = -1, \chi_+ = 5, \chi_- = 2, \gamma_+ = 1, \gamma_- = 1, \Lambda_+ = 2, \Lambda_- = 0$; Initial values: $\rho_s = 0.031, \alpha_+ = 0.20272, \alpha_- = 0.2, l_+ = 1, l_- = 1, \rho_+ = 0.597, \rho_- = 0.239$.) Note that here u and w are plotted logarithmically.

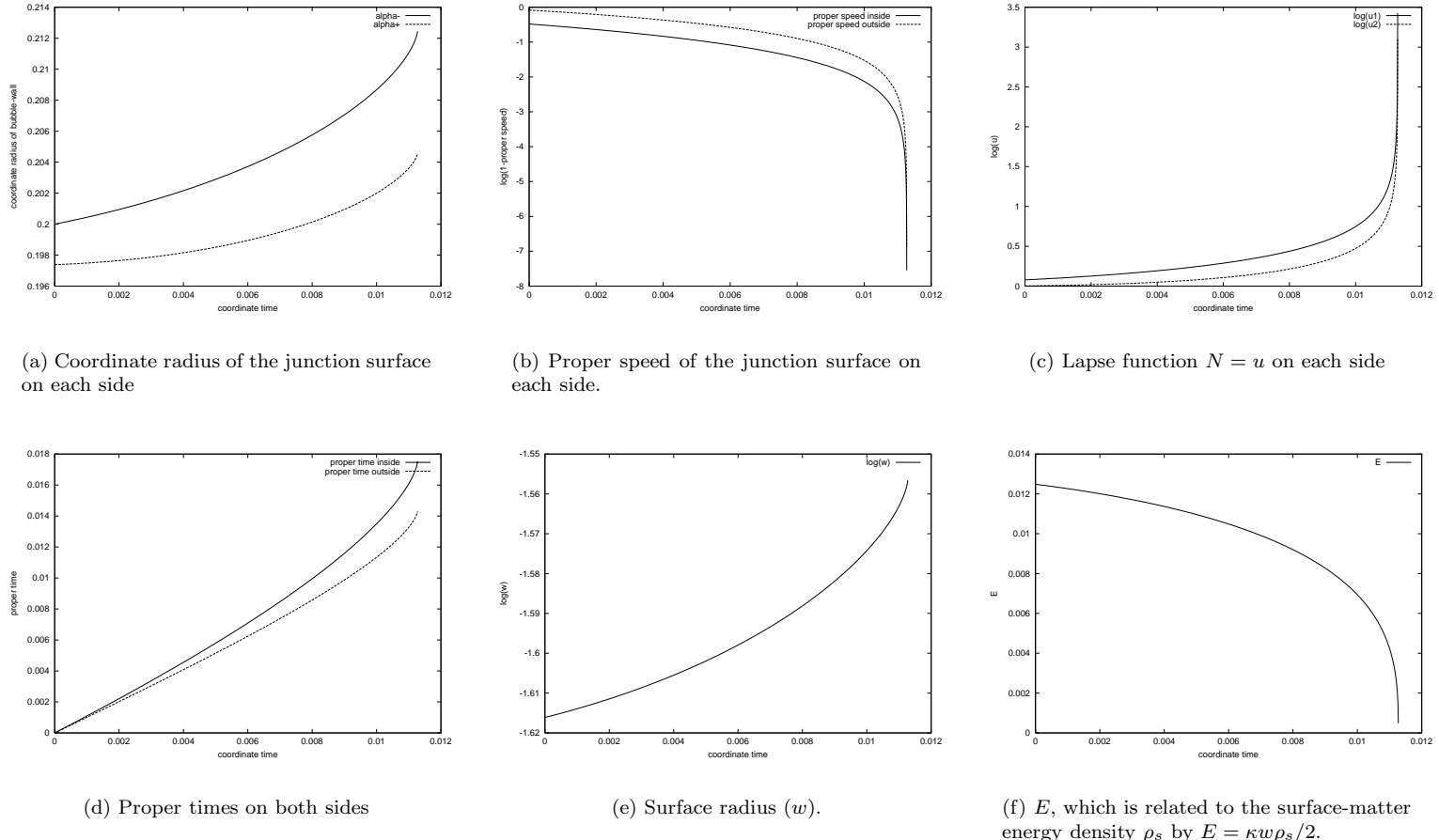


Figure 9: Evolution of a junction between a closed (inside) and an inflating open (outside) geometry. The inside has a radiation equation of state, while the outside is an inflating dust model. (Parameters: $\gamma_s = 1, \zeta_+ = -1, \zeta_- = +1, \chi_+ = 0, \chi_- = 1, \gamma_+ = 1, \gamma_- = 4/3, \Lambda_+ = 5, \Lambda_- = 0$; Initial values: $\rho_s = 0.005, \alpha_+ = 0.19739, \alpha_- = 0.2, l_+ = 1, l_- = 1, \rho_+ = 0, \rho_- = 0.119$.) Note that here u and w are plotted logarithmically.

The behaviour for small values of $E = \kappa w \rho_s/2$ has been investigated. It was shown that for certain cases E is driven to zero within a finite coordinate and proper time. At such a point our formalism breaks down. Nevertheless, we want to speculate here that in such cases the junction really turns spacelike. This can be seen as an inadequacy of the thin wall formulation in such situations — a causal propagation of a discontinuity should not exceed the speed of light. We suggest that in such cases the spatial extent of the transition region is not negligible.

The developed formalism gives us two sources for constraints on possible junctions. Firstly the time derivative of the surface radius is given by the quadratic equation (30). Demanding that real solutions to this equation must exist directly restricts the possible values of the surface energy density for a particular junction (see figure 2). Secondly, in our approach physical solutions must have a lapse function which is greater than or equal to unity. The resulting restrictions depend on the metric components on each side of the junction — they either determine the sign of the derivative of the proper surface radius, or they restrict the possible surface-energy densities (see figure 3). For the latter case the allowed ranges for $E = \kappa w \rho_s/2$ have been given explicitly.

For the special case of junctions between FLRW models with γ -equation of state it was shown that alone on geometrical grounds there can be no comoving junction surface — whether with or without surface layer.

As a particularly simple and well-known case, ‘vacuum bubbles’ were discussed. and the results agree with the literature. A particularly interesting model, the junction between an empty, open, inflating FLRW region outside and a radiation dominated closed FLRW model inside, has been investigated in more detail. The inside region re-collapses after some finite proper time and hence the junction surface has to be terminated. Besides a disappearance or a detachment of the closed inner region we suggest that the junction can turn spacelike — an effective disappearance of the outer region.

This and other examples have been integrated numerically. It was observed that many models seem to reach the speed of light within a finite *proper* time, in accordance with the predictions from section 2.6. Since a spacelike junction violates causality, we suggest that a breakdown in the thin-wall approximation must have occurred.

Our results show that the thin-wall treatment of timelike junctions (without the presence of scalar fields) is on a *mathematical* sound level. Nevertheless, in many cases the junction surface reaches a singular point within a finite proper time. We believe that in these cases the thin-wall is not a *physically* acceptable approximation.

References

- [1] Spergel D N *et al* 2003 *Astrophys. J.* (*Preprint* astro-ph/0302209)
- [2] Guth A H 1981 *Phys. Rev. D* **23** 347
- [3] Linde A D 1983 *Phys. Lett. B* **129** 177
- [4] Linde A D 1990 *Particle Physics and Inflationary Cosmology* (Chur:Harwood Academic Publishers)
- [5] Lanczos C 1922 *Phys. Zeits.* **23** 539; and 1924 *Ann. der Phys.* **74** 518
- [6] Dautcourt R 1964 *Math. Nachr.* **27** 277
- [7] Israel W 1966 *Nuovo Cimento B* **44** 4349
- [8] Blau S K, Guendelman E I and Guth A H 1987 *Phys. Rev. D* **35** 1747
- [9] Berezin V A, Kuzmin V A and Tkachev I I 1987 *Phys. Rev. D* **36** 2919
- [10] Lake K 1987 in *Vth Brazilian School of Cosmology and Gravitation*, Ed. Novello, World Scientific, Singapore, pp1-82
- [11] Hájíček P and Bičák J 1997 *Phys. Rev. D* **56** 4706-19 (*Preprint* gr-qc/9706022)
- [12] Sakai N and Maeda K 1994 *Phys. Rev. D* **50** 5425-5428 (*Preprint* gr-qc/9311024)
- [13] Misner C W, Thorne K S and Wheeler J A 1973 *Gravitation*, W. H. Freeman and Company, San Francisco

- [14] Coleman S and De Luccia F 1980 *Phys. Rev. D* **21** 3305
- [15] Jensen L G and Steinhardt P J 1984 *Nucl. Phys. B* **237** 176-188
- [16] Lyth D H and Stewart E D 1994 *Preprint* hep-ph/9408324
- [17] Amendola L *et al* 1996 *Preprint* astro-ph/9610038